كلية الهندسة بشبرا
FACULTY OF ENGINEERING AT SHOUBRA
ERJ
PRINT ISSN 3009-6049
ONLINE ISSN 3009-6022

ENGINEERING RESEARCH JOURNAL (ERJ)
Volume (53),Issue (1)
January 2024, pp:117-129
https://erjsh.journals.ekb.eg

Evaluating groundwater potential through GIS technique for Sadat City, west Nile Delta, Egypt

Ahmad A.Elsattar [1,*], Manal A.Moneam [2], Elzahry Farouk [1], Neveen B. Abd EL Meged [1]

[1] *Faculty of Engineering at Shoubra, Benha University, Cairo, Egypt.*
[2] *Research Institue for Groundwater, NWRC*
**Corresponding author*

E-mail address: ahmadpublic94@gmail.com, manal338@hotmail.com, elzahry@hotmail.com, nevine.badawi@feng.edu.eg

Abstract: Groundwater is a sacred source of water in Egypt and is considered a pillar for any project in the desert area. Due to the continuous reclamation projects for the desert water, it is required to carry out evaluation studies for the aquifers being used to monitor and evaluate its conditions for any risks. Such evaluation studies require the use of both GIS techniques and Numerical models to evaluate the whole aquifer. This paper presents an evaluative approach to discuss the potential of groundwater in Sadat City. The core of this research is using GIS techniques and Numerical modelling to determine the current state of the aquifer. The GIS techniques are used to feed the Numerical models with the required inputs. Numerical models were used to give a close insight to the study area hydro geologically in 1990 and 2017. The Numerical models were calibrated in 1990 to start the calibration in the steady state of the aquifer. Another calibration was done in 2017 for the transit state to calibrate the current state of the study area. After ensuring that the models accurately simulate the aquifer. 3 different scenarios were implemented on the model to see the reaction to each scenario. The different scenarios showed a huge depression of groundwater levels in 2025 and 2030 but with different levels according to each scenario. Chemical analysis was performed on 4 water samples within the study area. A potential map was created based on a qualitative approach and the previous findings for the study area in 1990 and 2017 to conclude the results of the study area. High numbers of TDS (around 3000 ppm) were found in the large extraction areas in the south border of the study area as well as the adjacent parameter between the Quaternary aquifer and Wadi-Natrun aquifer in 2017. Due to the obtained results, the eastern side of the study area became a moderate potential aquifer and the rest of the aquifer became a low potential aquifer.

Keywords: groundwater evaluation; potential maps; ancillary analysis; GIS techniques.

1. Introduction

Since the start of spatial analysis and visualization using computers by Michael Goodchild in 1960, water studies have gone hand in hand with GIS techniques to facilitate the modelling process. USGS and the Connecticut Department of Environmental Protection started a joint project to model water resources in 1985 and arguably the first-ever groundwater model. Later in 1995 [1] presented the first guide to use GIS in conceptualizing groundwater systems. In Egypt [2] in 2005 presented a use of GIS techniques in groundwater management for the western Nile Delta.

All these studies showed different types of coupling GIS and numerical modelling in studying water resources. The first approach is loose coupling in which the inputs of numerical models are processed by GIS and then fed to numerical models. After turning those to outputs they are presented in GIS software to a spatial dimension to the outputs to help decision-makers. The second approach is the tight coupling of both GIS and numerical models. Such as numerical modeling by simple equations in the GIS environment or using scripting languages to code advanced mathematical equations inside the GIS software and final approach is by using a wrapper program that can call both functions from each software and visualize the results of each program in the same interface.

Creating a conceptual model is the ability to create a simplified idea of how the model behaves. The Sherman model in the 20th century was the first to describe the rainfall catchment using a unit Hydrograph. In 1925 Theis was the first to give a valid mathematical model of a groundwater phenomenon that is groundwater flow to a well under specific conditions. After finding a reasonable and sensible idea to describe the system, finding the mathematical equation to describe the system is the following step.

Data-driven models are used to obtain the numerical formulas that are needed to describe a phenomenon. Based on observations between a set of inputs and a set of outputs. Usually, this kind of model is used within economics and social science with the help of linear and logistic techniques. The emerging developments in artificial neural networks are being used to enhance the accuracy of the results achieved.

Physical-based models are based on the use of fundamentals of physics just as the law of conservation for mass, momentum, or energy. The mathematical equation found from this model is used to give an understatement of the process being discussed and describe the process and interaction between inputs and outputs. Those mathematical formations take multiple formulas from ordinary to partial formulas. Assumptions are being used to facilitate finding the governing equation. Numerical models are used to approximate the solution. The use of numerical models helps build computational algorithms to facilitate the modelling process.

Expert-driven models are based on the experts' experience and their judgment. Such models are preferred whenever the other types of models are impossible to develop and give reasonable outputs. In such models, the stakeholders participate in multi-criteria decision-making meetings. Such models provide long-range and narrow-down predictions.

Building a conceptual model determines the set of parameters governing the numerical model and allows it to converge to find the solution. The physical framework that happens inside the phenomenon must be described. In groundwater modelling, topology, and drainage networks as well as water tables are an important set of factors that must be included in any groundwater model. Hydrological parameters must be included and described with great care in the conceptual model. Hydrological parameters manage to describe the interaction between the discharge systems, surrounding boundaries and the whole water cycle. Any mistake in such parameters affects the whole model outputs. Chemical parameters manage to uncover the potential threats to the groundwater system. Also, the chemical parameters play an important role in defining the safest places to invest for reclamation. [3] It found that Sadat City's groundwater system is an unconfined aquifer and is affected by surface water. [4] In 2005 a numerical model for the western Nile Delta using Modflow. Such models are based on Darcy's law which is illustrated below.

Darcy's law for the movement of fluids was used to understand the groundwater flow in a porous material as follows:

$$\boldsymbol{S_s}\,\frac{\partial h}{\partial t}=\frac{\partial}{\partial x}\left(K_{xx}\frac{\partial h}{\partial x}\right)+\frac{\partial}{\partial y}\left(K_{yy}\frac{\partial h}{\partial y}\right)+\frac{\partial}{\partial z}\left(K_{zz}\frac{\partial h}{\partial z}\right)-w$$

Where:

- x,y,z are the cartesian coordinates aligned along the major axes of the hydraulic conductivity Kxx , Kyy and Kzz
- h is the potentiometric head
- w is a volumetric flux per unit volume and represents sources and/or sinks of water
- S is the specific storage of porous material.
- T is time

In addition to the previous formula with boundary conditions, it is possible to construct a numerical model to understand a groundwater system [5].

2. Material and methods

2.1 Methodology

The methodology we used in this study was used before in studying the western Nile Delta and creating a potential map in 2007 [6]. The result of that study suggested monitoring the western Nile Delta to alert any risk arising from the extreme use of groundwater and how it affects the aquifer and the environment. In this study, we continue using it and focus on a small area within the western Nile Delta. We used the loose coupling of GIS and Numerical modelling. So, we can prepare the inputs of the Numerical model by the GIS and then take the outputs of the Numerical model to present them in GIS format as a groundwater potential map. After that, chemical analysis was performed for four samples within the study area to give us an understatement of the quality of water within the study area.

2.2 Study Area (Hydrogeology, geology, and geomorphology)

Sadat city is the first of many cities that was built in Egypt to escape the very crowded river Nile Valley. The city is located 80 km north of Cairo along the Cairo-Alexandria Desert Road. Due to the location outside the main valley, groundwater was used to start the city construction and the mixed use of groundwater and surface water was used as the source of water for irrigation and domestic use. The Quaternary aquifer is the main aquifer under Sadat City and west Nile Delta. The Quaternary aquifer has a thickness of 200 mt 900 m. It's a semi-confined aquifer. The slope of the aquifer clay base is 4m/km which is 40 times the surface slope. During the Quaternary Age water formation was formed. Two major formations in the Quaternary aquifer. During the Pleistocene age, the Mit Ghamr formation was created. During the Holocene age, the Bilqas formation was created. Sadat City consists of old alluvial plains on the surface. Pleistocene-graded sand and gravel with clay lenses are below the old alluvial plains. Pliocene deposits consist of alternating layers of sand and clay with limestone at the top of it. The Pliocene deposits work as aquiclude as it has Pliocene clay below the surface. The Quaternary aquifer base is around 100 meters below the surface and the Miocene base is around 300 meters.

Another major aquifer in the western Nile Delta and very close to the study area is the Moghra aquifer. The Moghra Formation is the main formation in the Moghra aquifer. It is characterized by Miocene sand and sandstone interspersed with clay. The aquifer is covered with Oligocene basalt and shale which is underlain by Pliocene basalt in the southern and western parts of it. In the remaining areas, it is visible at the surface and experiences some restriction from the interbedded clay layers in both the northern and eastern parts. The two aquifers are separated by Pliocene deposits except for the distance along Khatatba-Abu Rawash Road and Sadat City- Khatatba in which they are connected vertically.

The surface geology in the study area contains different formations. 1) El-Hagif formation: which is marl and lenses of limestone. 2) Gabbal Khashab: petrified wood and conglomerate distributed in dark brown sandstone. 3) Protenile sediments: fine sand, clay and silt deposits. 4) Prenile deposits: sediments that existed before the Protenile sediments 5) Stabilized deposits: flat and stable dunes of fine sand 6) Nile silt: the Nile silt that come with the floods 7) Sand dunes: longitudinal quartz-rich sand aggregates. 8)

Sabkha deposits: silt, clay and evaporate deposits 9) Wadi Deposits: superficial layer of gravel and sand with clay.

The subsurface geology is characterized by rocks from the late Cenozoic era. The main two periods that made up the rocks of the study area are the tertiary era and the Quaternary era. They created old rock fragments. The Triassic epoch consisted of the Pliocene, lower Miocene, and Oligocene sub-epochs. The Quaternary period has the Holocene and Pleistocene periods. The Holocene formations are 1) the first formation consisting of sand dunes and surface sediments, air deposits derived from previous rocks. 2) Second formation facies sediment made up of salty silt deposits of brine water evaporation 3) third formation which sandy clay and its facies of 30 m tick that can be found in Nile Delta plains 4) fourth formation is a deformed Quadrilateral unit that consists of facies if valley and fan shaped alluvial sediments. The Pleistocene era was a single rocky unit of sand and gravel with clay lenses.

The geomorphological setting of the study area has 2 formations and 2 alluvial plains. The new alluvial plains lay over a silt clay layer and were full of canals, drains and villages. The old alluvial plains are known for their smooth slope toward the superficial drains. Fanglomerates which are the wadi washes that are carried by the drainage system and dumped in shallow depressions. Last is the well-developed traverse sand dunes which consist of long bars of loose sand on both sides of the Nile Delta.

2.3 Study area geographically

The study area is within the western Nile Delta. The study area is 80 km from Cairo along the Cairo Alexandria desert road. Sadat city is inbounded by (30° 17’, 30° 24’) and (30° 36’, 30° 42’) (lat, long) respectably. The West Nile Delta is bounded by the western border with basalt superficial. Sadat city itself exists above the Pleistocene gravel and graded sand that’s intercalated with clay lenses [7]. Below the surface layer lies the Pliocene deposits with limestone at the top and alternating sand and clay below it. An Aquiclude layer of Pliocene age is below the surface at about 600 meters MSL. The base of the Miocene aquifer is around 300+ meters under the city. The base of the Quaternary aquifer is about 100 meters below the city's surface. Groundwater is found between 40 to 80 m under the city. Aquifer production is known for its moderate productivity. The city's reclaimed areas for cultivation are based on irrigation from groundwater.

The Western Nile Delta has been known for its arid desert for generations and is an abandoned area. In the 1950s some minor projects to reclaim land based on surface water. Then in 1990 projects ran by the government started to reclaim 400 000 fed and followed by 100 000 feds after. Groundwater has been used to reclaim the desert since 1985. A mixed-use of groundwater and surface water was implemented as 180 million m3/year of groundwater was extracted with surface water to reclaim land in (Bustan, Tahrir). 460 million m3/year of groundwater was extracted to reclaim land east and south of Wadi Natrun [8]

The study area spans from 534884 m to 583045 m and from 847000 m to 884159 m. with a fault from the center of the south boundary to the center of the center of the western boundary. The group of canals extends in the northeast and northwest of the study area. The Quaternary aquifer bed varies from -100 from the southwest to -300 in the northeast. The topography varies from 20 m to 40 near the fault with some hills around 50s and 60s. A huge depression between the fault and the southwest corner of the study area and a bigger hill right at the southeast corner about 80 m above sea level. The Miocene aquifer lies below the Quaternary aquifer to a depth of -400 m below the sea level. But since it acts as Aquiclude it was not added to the model. There are 3 parts within the study area. Each part has a different productivity from the other part according to [8]

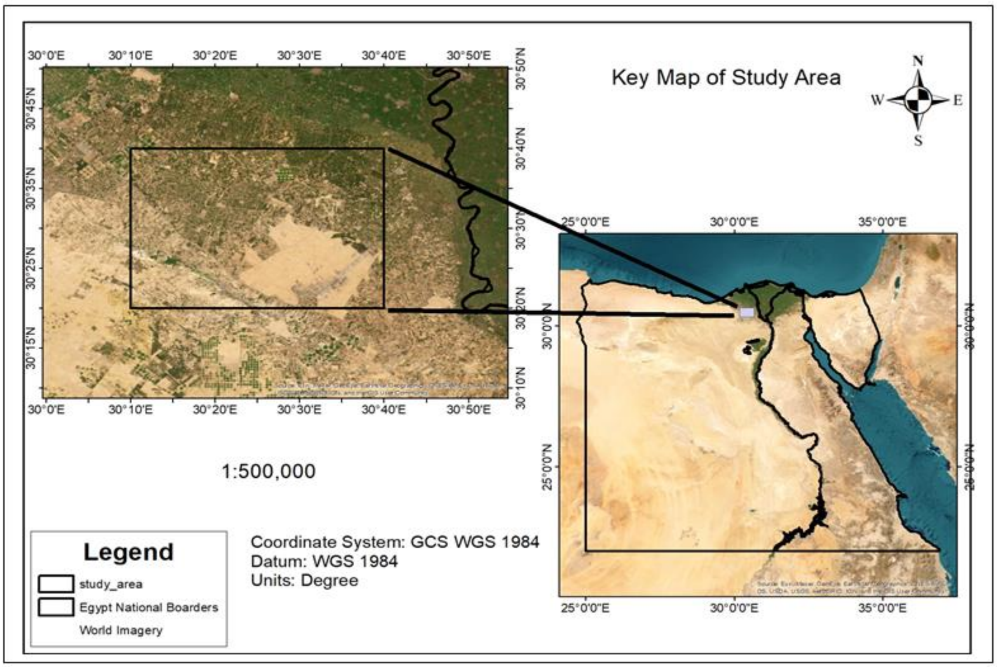

Figure 1 location of study area scale 1:5000000

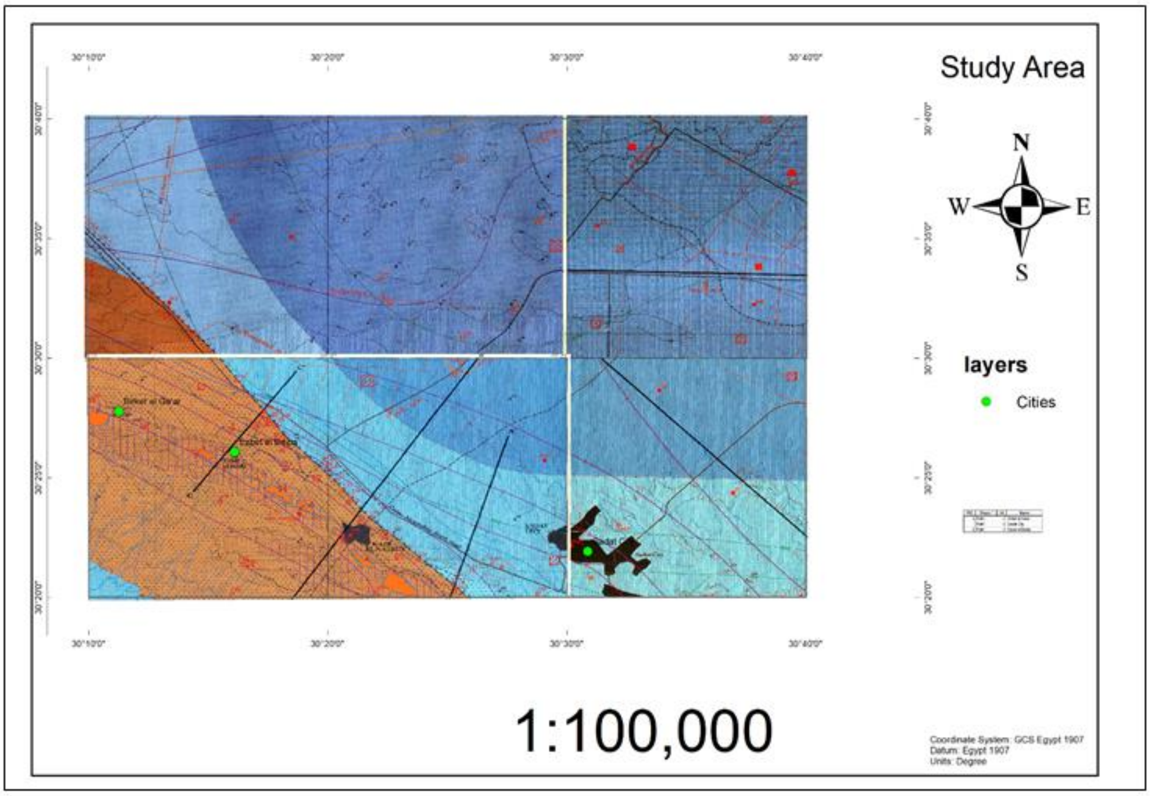

Figure 3 Hydrogeologic map of study area

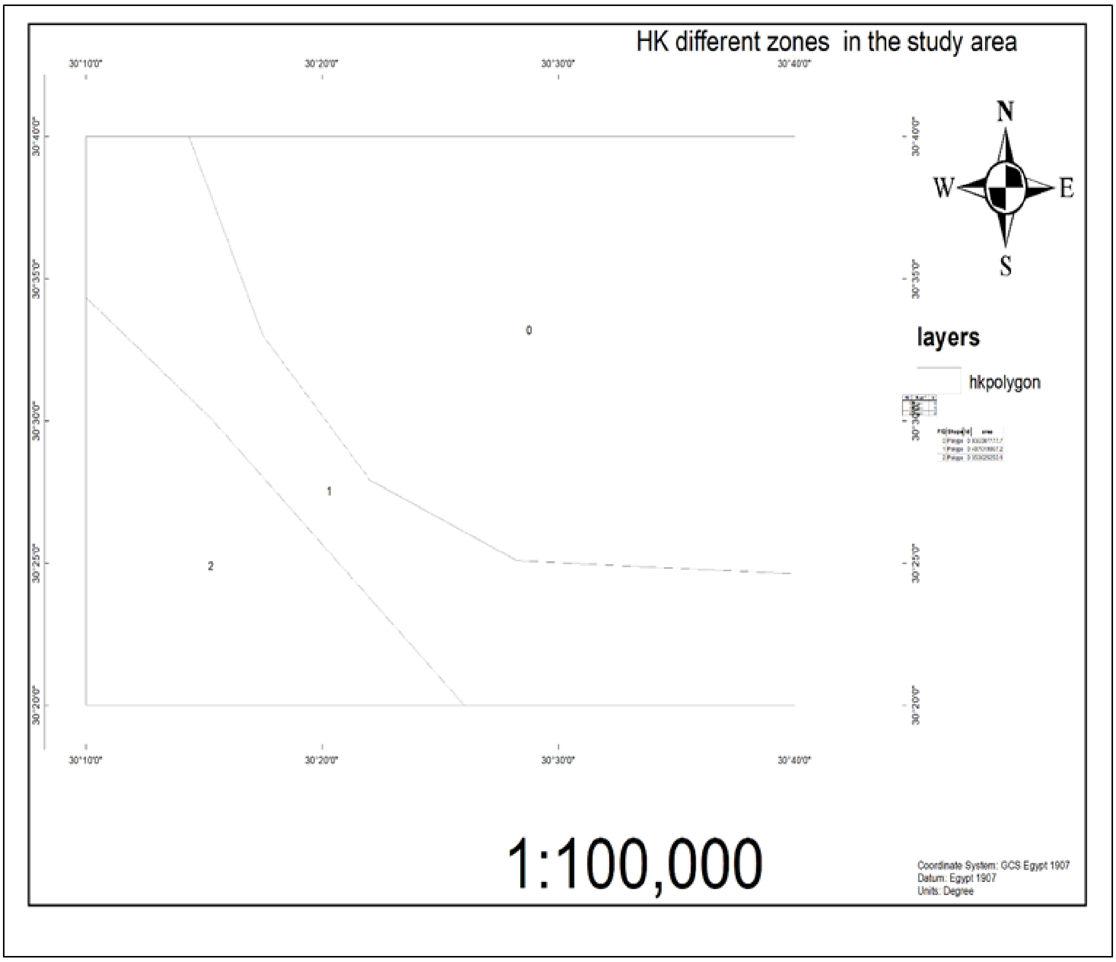

Figure 4 different hydraulic zones in the study area

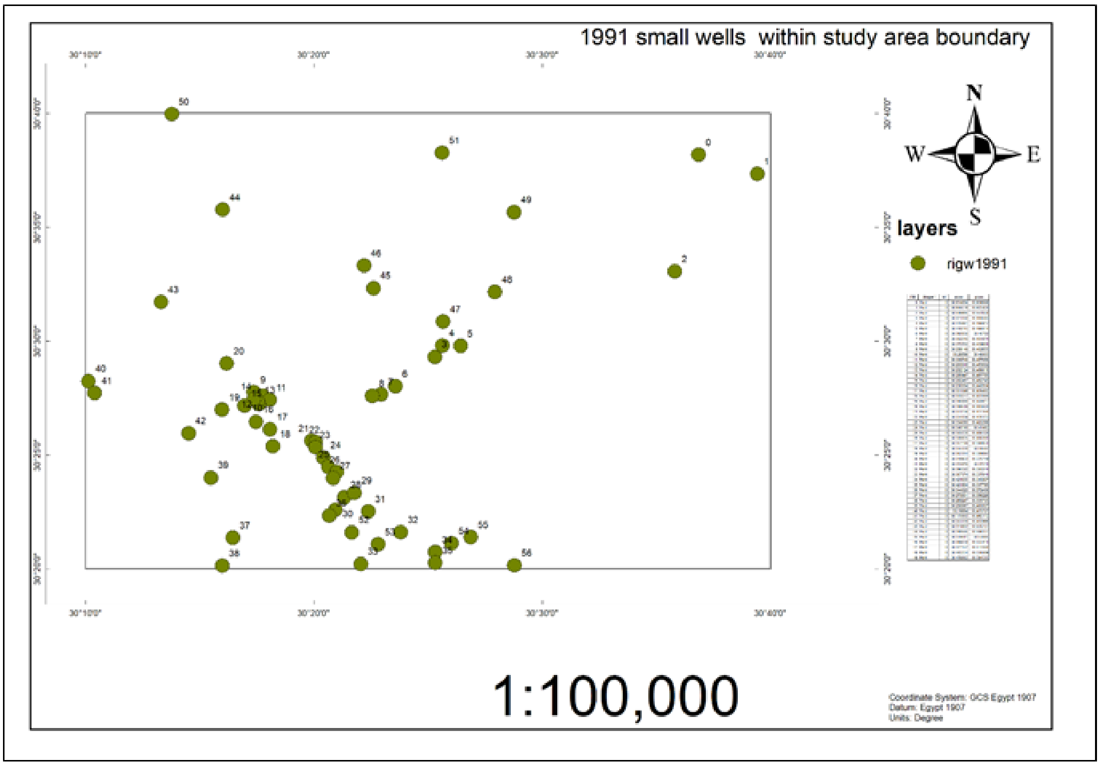

Figure 5 small wells in the study area in 1991

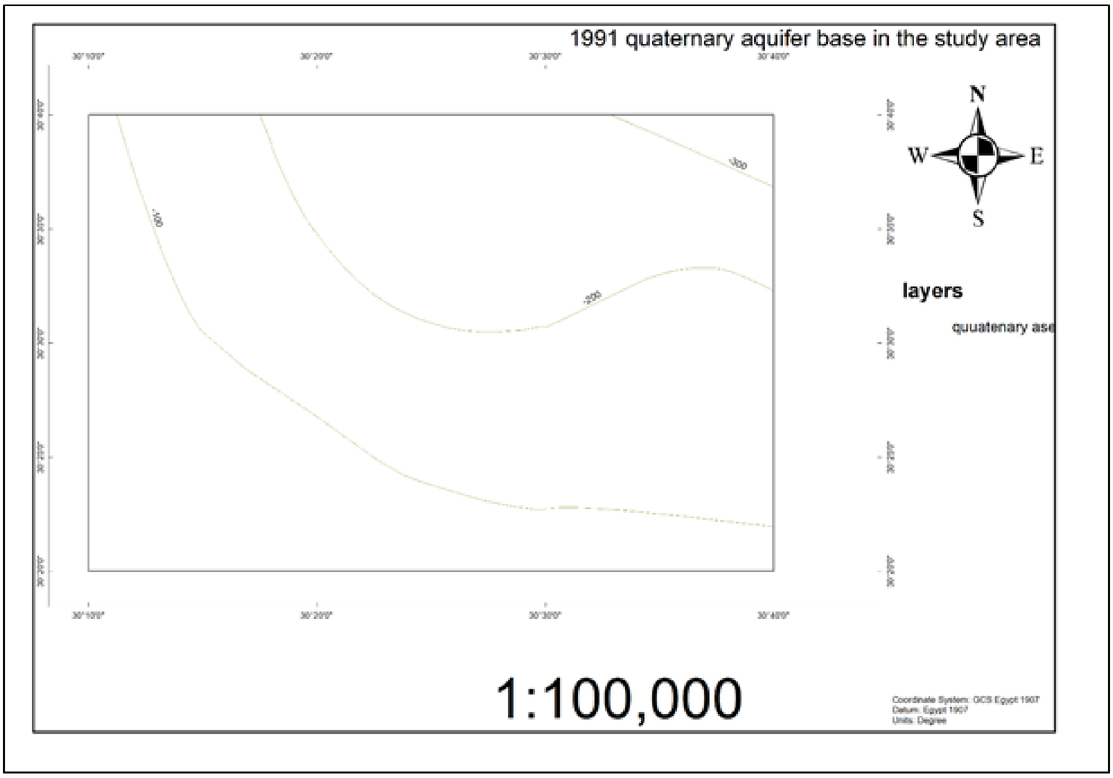

Figure 6 Quaternary aquifer base

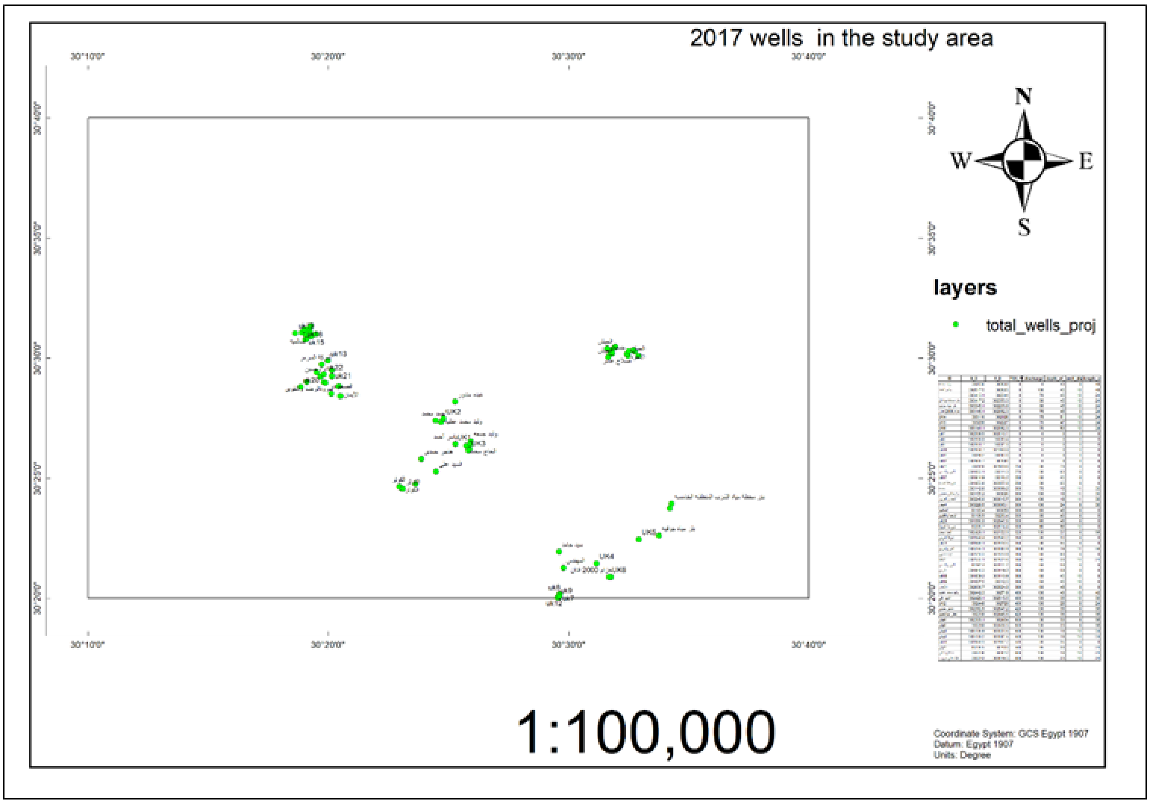

Figure 7 Wells in the study area in 2017

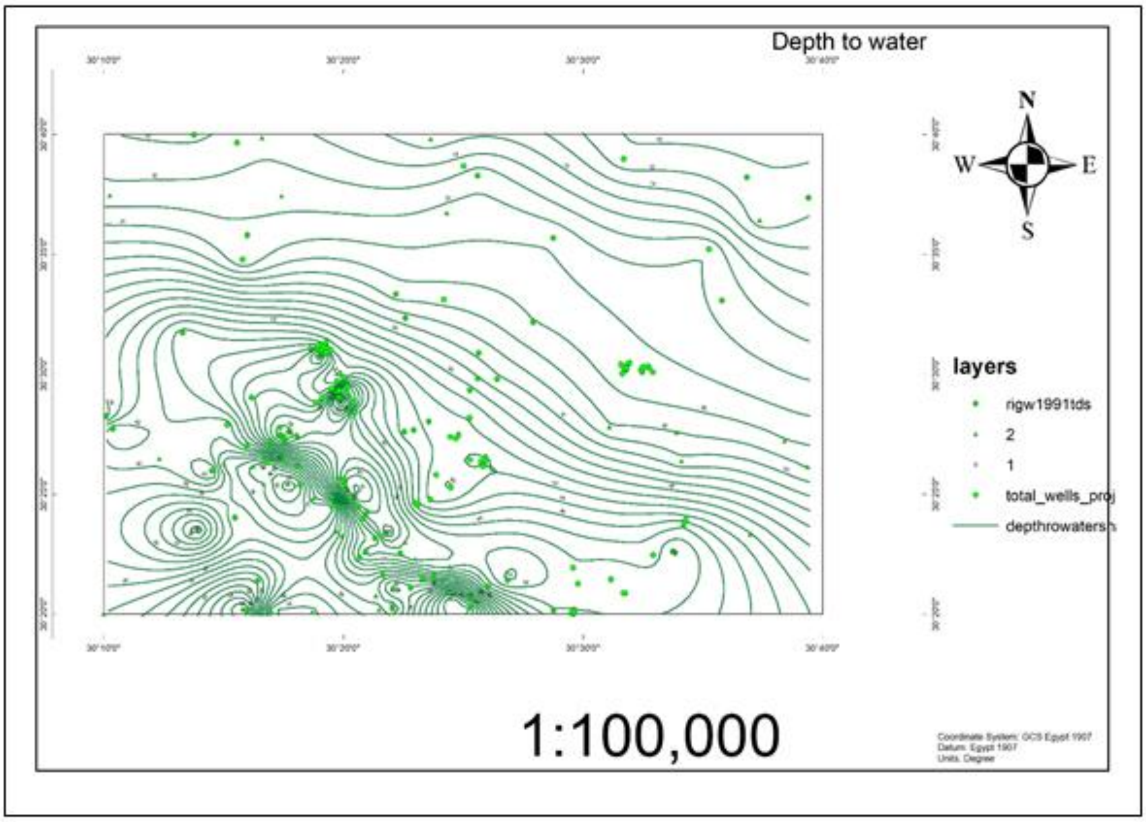

Figure 8 depth to water

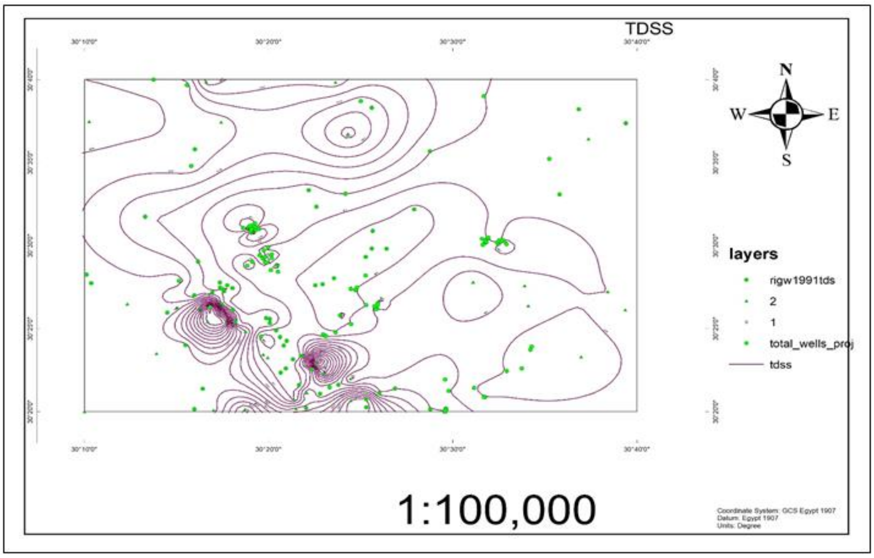

Figure 9 TDS

Sadat City lies in the south of the study area where the moderate productivity aquifer expands. Ezbit el Baid and Birket el Ga'ar expand over the Wadi Natrun aquifer western of the study area. The three different zones of productivity and hence hydraulic conductivity are seen in the Hydraulic conductivity map. The eastern zone has high productivity and is known for its graded gravel nature and cement with inter lenses of clay also being recharged from the infiltration of canals. The middle zone only recharged from surface rains which is neglectable. The Western zone is a low-permeable aquifer. The aquifer is recharged by the water movement from the surrounding aquifers. It was formed during the Tertiary and Quaternary eras.

The wells inside the study area were taken from the 1990 wells inventory. They are mainly located in Wadi Natrun aquifer which is known for being a low permeability aquifer. The eastern boundary in the study area is focused on irrigation by surface water which is why there are fewer wells than the western boundary. Another group of wells were identified in 2017 with different types of data like length of screen, depth of water, discharge, TDS and well diameter. Those wells were used to develop a transit model and helped build salinity maps and depth to water map of the study area. It was easy to develop depth to water maps based on the well's inventory of 1990 and 2017. The majority of west Nile Delta is suitable for drilling wells as the groundwater can be found within a few meters in some places to around 200 meters in the south desert road at kilometre 46 as the drilling penetrates the Oligocene formation. In different places and due to continuous extraction, the groundwater got deeper over the past decades such as Dina Farms, and Wadi El Faragh. In other places, a water logging issue occurred as the depth to water got shallower. It is important to understand the spatial dimension of the TDS in any area as it affects both human beings and plants. Some areas between the Rosetta branch and Wadi Natrun have higher TDS because the rock minerals dissolve the water. The groundwater in the Wadi Natrun is brackish. Other places like Dina Farms, El-Khatatba Road (4.8mm);

2.4 Data collection

The data collected was grouped into 3 categories:

- 4 hydrogeological maps in 1990 [9]–[12] that contained all the hydrogeologic characteristics of the study area from groundwater levels, depth to water, land use etc. Those maps provided us with a basic understanding of the study area. The data in those maps helped us build a 3D model of the study area. The topology extracted was used in building the surface of the grid. The bottom of the top aquifer was used to build the bottom grid. The piezometric levels are used in starting the static calibration of the static model. A map of TDS was created from that map to show the suitability of water within the study area. A map of depth to water was created from this map to show the drilling depth to water.
- Wells data within the study area. Those data wells are categorized into 3 different types.
  - The first is the pumping test and recovery test of 4 wells in the centre of the study area and they were analyzed according to [13]–[15] [16] ,[17], [18]to capture the hydrogeologic parameters of the aquifer as transmissivity, hydraulic conductivity and storativity. Those numbers were later used in building the numerical model and provided with the start numbers for calibration.
  - The second inventory is the data from 1990 which were a group of wells found in the hydro geologic maps. Those wells were assigned with discharge from the discharge maps on the hydrologic maps mentioned above.
  - The third inventory is a group of wells in 2017 of wells that were drilled in the aquifer during the period from 1990 to 2017. The inventory contained data on discharge, TDS, screen depth, well depth and other data used to model those wells in the Numerical model.

- Water samples that were taken from wells in the study area and were later used to give an understatement of the nature of the water and its suitability for both irrigation purposes and domestic use purposes. Different types of chemical analysis were performed on the water sample to understand the nature of water quality within the study area.

3. Results and Discussion

3.1 Numerical modeling

The Kriging method was used to interpolate the data layers from the previous work on the hydrological maps. After creating layers of data for the topography, piezometric levels and base of the quaternary aquifer. Building a numerical model using GMS with a mesh of 250*250 m to represent the model area which is close to 48 km*36km. a steady-state model was created for the study area. The model was used to represent the current state in 1990. Calibration was performed to assure the stability of the model and match the simulated data with the observed data. The results showed high accuracy and less than 5% error between the observed and simulated data. Also, a little difference was observed between the inflow and outflow from the system which is about (-4.6*e-8).

The transit model was created to calibrate the model with the observed data in 2017 with simulated data from the model. A different set of observed data was used to calibrate the model. A new set of wells was added to the model. Updated the extraction data of the whole wells. The same hydraulic parameters were used. After multiple iterations, the model converged the model and stimulated the same data observed with the same standard deviation as the steady state.

3 different scenarios were used to predict the state of the study area in the future (2025 &2030). The first scenario was to continue the extraction with the same values without change. It showed an additional drop in the piezometric levels by at least 3m and increased the radius of effect. The second scenario was to increase the extraction rates by 20%. In this scenario the dropdown increased by 13 m and the radius of influence increased. The third scenario was to reduce the extraction rates by 20% which didn’t increase the dropdown by much, yet it kept the radius of influence from a wide increase and affected a lot of the study area. The current state and continuing at the same speed shall harm the aquifer and reduce the ROI for any investment as the initial cost increases rapidly with the deterioration in the drawdown.

3.2 Groundwater potential

Groundwater potential is an indication of how much water can be pumped from the aquifer. The following factors help us determine the maximum amount of water extracted per location and the pumping head needed to extract the water over a period. [6] Groundwater Potential is based on different factors such as:

- Type of aquifer as extension and boundary conditions
- Aquifer recharge type and pace
- Hydraulic characteristics of aquifer
- Depth of groundwater
- Extraction of water

Those factors were analyzed and grouped according to their importance in the quantitative availability of groundwater [19]). TDS of groundwater plays a major role in the evaluation process. Groundwater extraction from local or regional aquifers, quality of recharge and land use /land cover are important factors in whether an area is suitable for reclamation or not [8]. A quantitative and qualitative analysis is performed on any area to determine the groundwater potential. In this study, a qualitative approach was used to determine the potential. The factors that were taken in this study are:

- Aquifers type, saturation and aquifer thickness
- Aquifer productivity
- Present and future groundwater depth
- Land use/land cover and extraction
- TDS

Those parameters were used to produce criteria to determine the potential and an integrated approach was implemented to produce the final potential map according to [20].

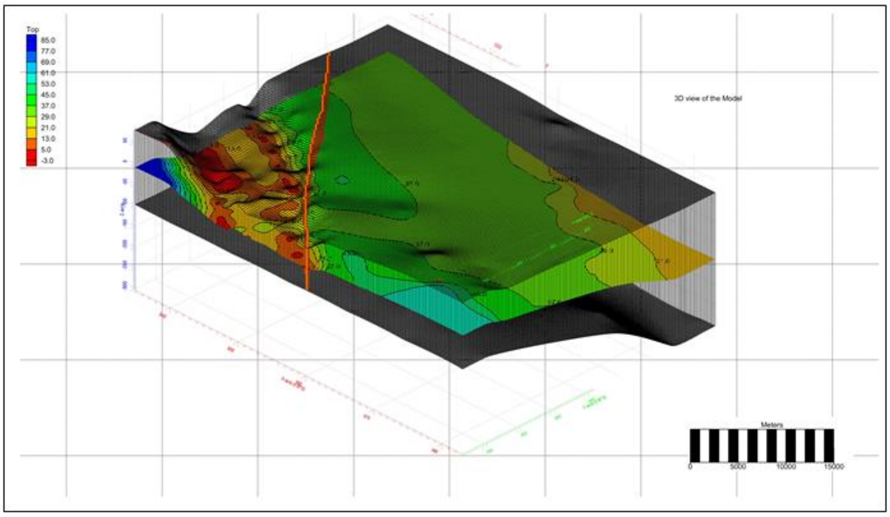

Figure 10 3D model of study area

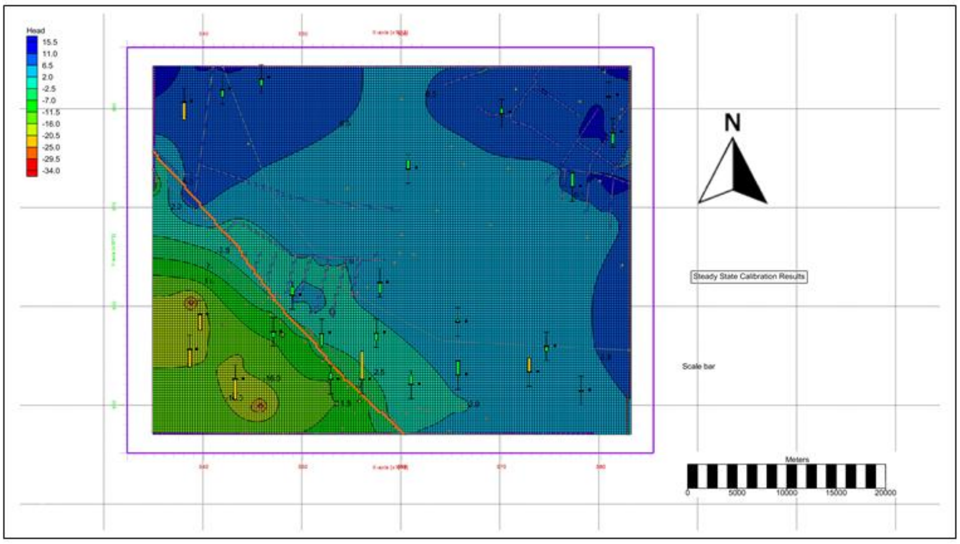

Figure 11 Steady State Calibration results

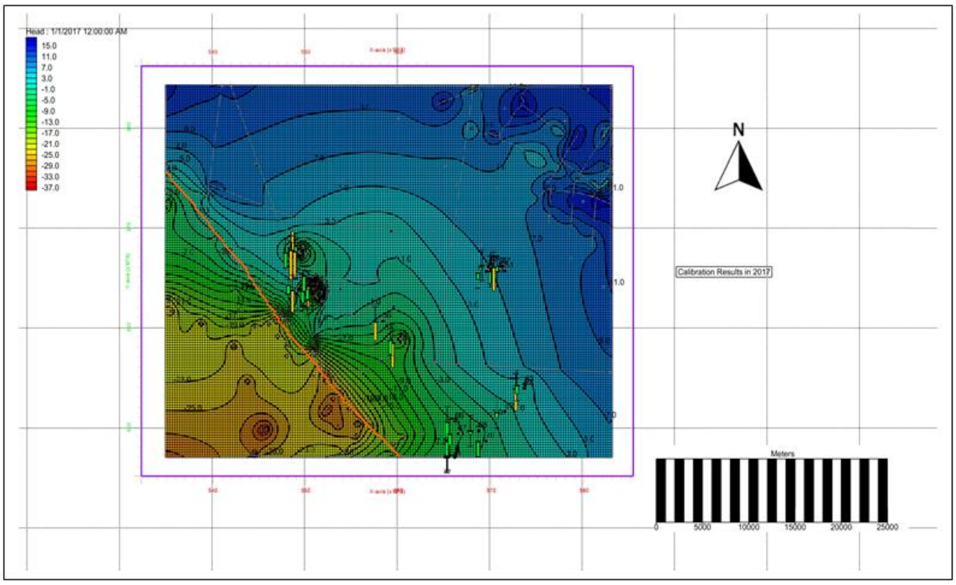

Figure 12 Transit data Calibration results

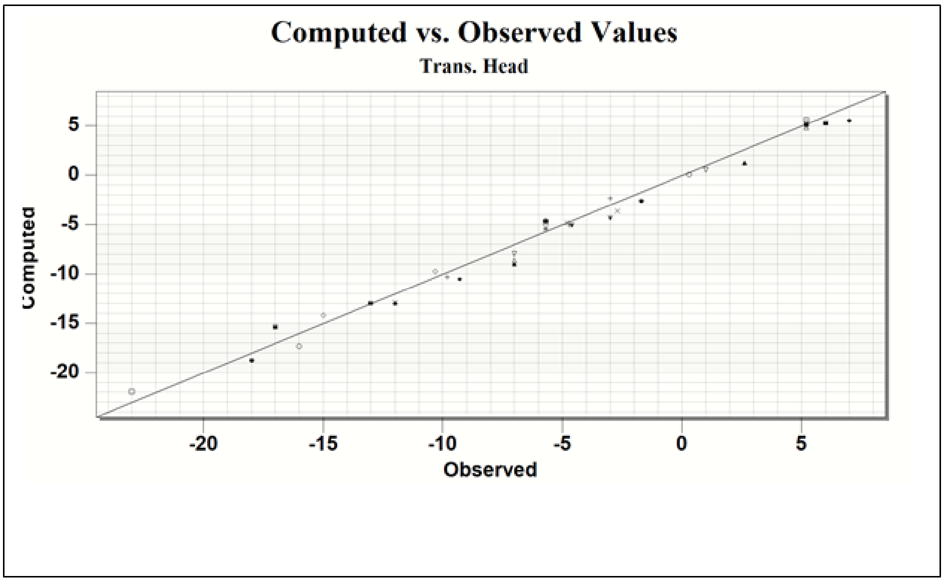

Figure 13 Observed vs Computed model results

TABLE 1. Classification criteria

Classification	Productivity (Cum/Hr/M)	Depth to groundwater(M)	Salinity (TDS) (PPM)
high	>50	<15	<1500
Moderate (green)	50-25	15-40	1500-3000
Low (Red)	25-10	40-80	3000-5000
None (Black)	<10	>80	>5000

TABLE 2. Integrated classification criteria

Classification	Productivity (Cum/Hr/M)	Depth to groundwater(M)	Salinity (TDS) (PPM)
High	High	High	High
	High	High	Medium
	High	Medium	High
	Medium	High	High
Medium	High	Medium	Medium
	Medium	Medium	Medium
	High	Medium	
	Low	Medium	Medium
Low	High	Low	Low
	Low	Medium	Low

3.3 Updated potential maps.

The concept of ground potential is that it assesses different parameters to help decision makers reclaim lands that give the highest ROI. In this study, a new methodology was used to assess the potential in 1990 and 2017. Using a potential cell-wise qualitative approach to produce a potential map. The study area was dissected into a grid of 6*8 km cell size that created a 48-unit cell. A density map of the annual extraction in 2017 was created according to the well inventory in 2017. That map was used to create a productivity map in 2017. Also, a density map for TDS in 2017 and depth to water in 2017 was created. The same maps were created for the 1990 well inventory.

Qualitative classification was created based on the criteria mentioned before.

3.4 Groundwater quality

Different types of sources of contamination for groundwater. Natural resources such as saltwater intrusion or the travel of ions or soluble salts due to the extraction from one place to another artificial resources such as accidental spills, contamination from agricultural activities or industrial activities. The artificial contamination is difficult to degrade or reduce its effect on the water quality. Septic tanks and leachate from landfills or industrial waste dumps contaminate local aquifers and are responsible for the wide spread of contamination to many local aquifers. 4 samples were taken from the study area. Those samples showed a reasonable number for total salt concentrations under 1000ppm which shows that the water is accepted for use in irrigation and drinking purposes. The analysis showed no nitrate contamination. Heavy metals are within limits for irrigation and drinking purposes. 3 of the 4 samples showed no microorganisms in them but only in the second sample were microorganisms. EC range was from 0.469 to 1.421 with an average of 0.773 which is considered slight to moderate according to [21]. The results of the cations and anions analysis showed that Na, Cl and SO4 are the dominant soluble in the sample which means that NaCl and Na2SO4 are the dominant salts. Different types of analysis were done on the samples such as the Wilcox division, Piper diagram and Schoeller diagram. The analysis indicated that the water is fresh water, no nitrate contamination, and heavy metals within allowable limits. No microorganism contamination. Water is accepted for use in irrigation with crops that are tolerant to salinity or semi-tolerant. It is advisable to use drip irrigation and consider irrigation before sunset.

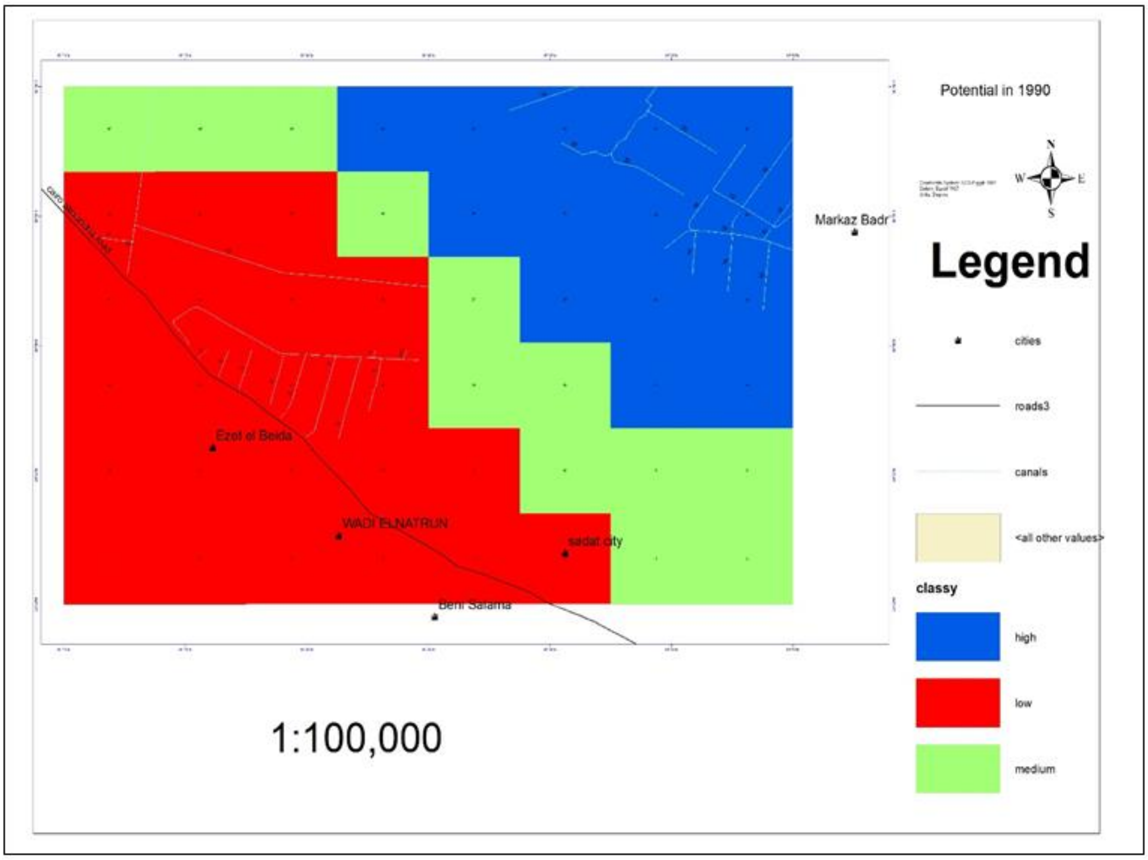

Figure 14 potential map of study area in 1990

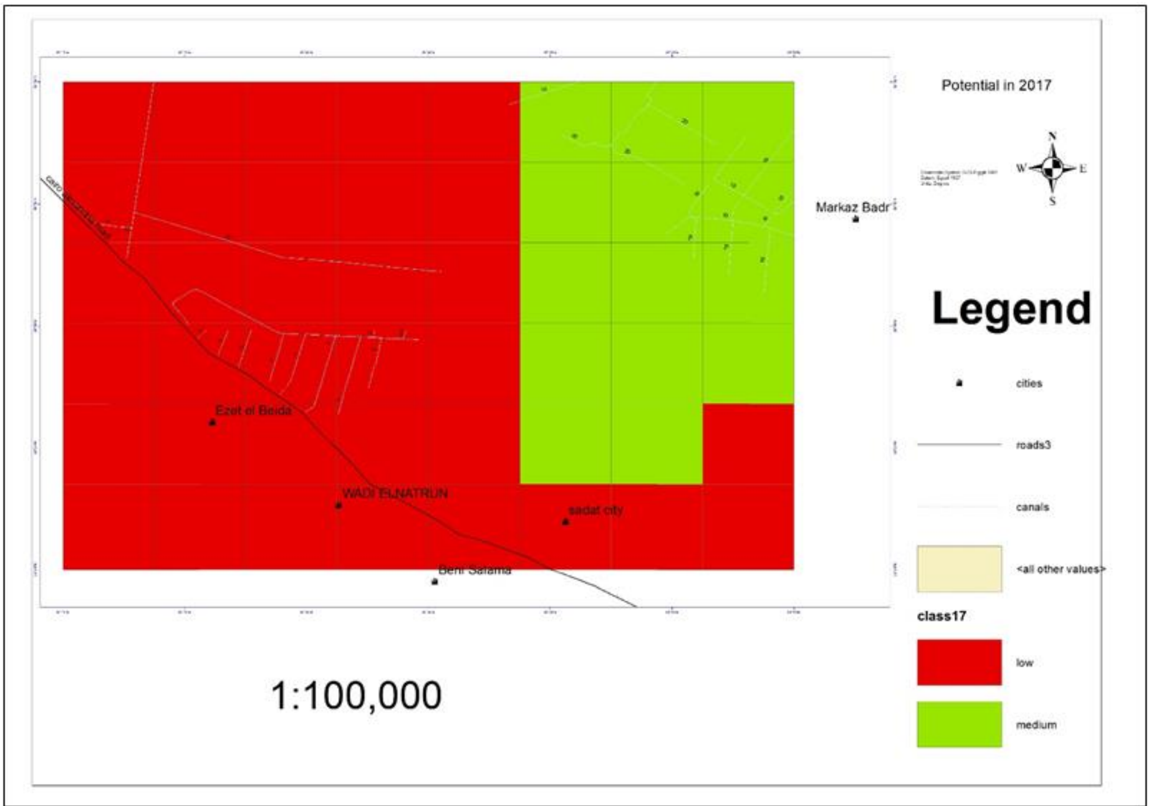

Figure 15 updated potential map of study area in 2017

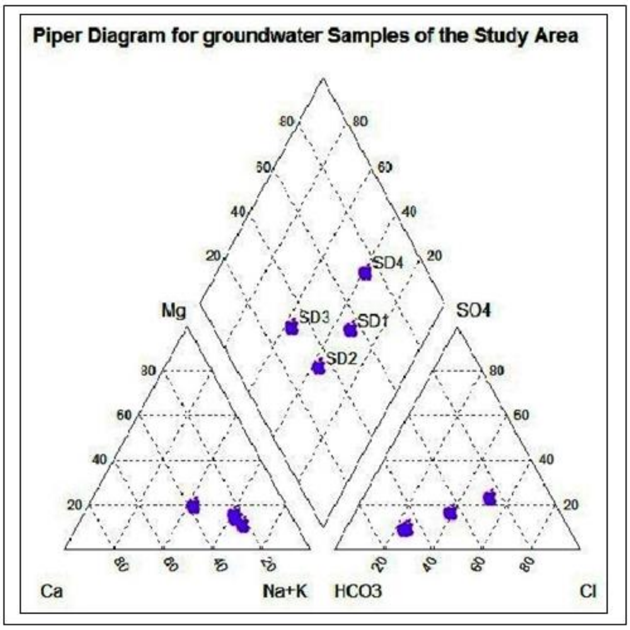

Figure 16 piper diagram

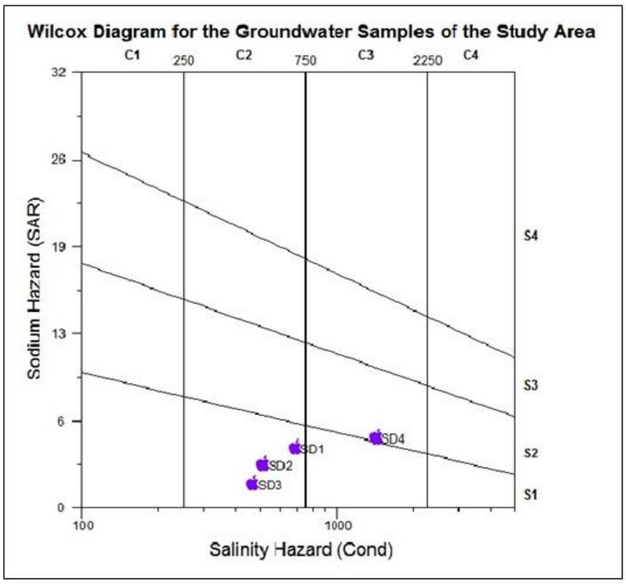

Figure 17 Wilcox Diagram

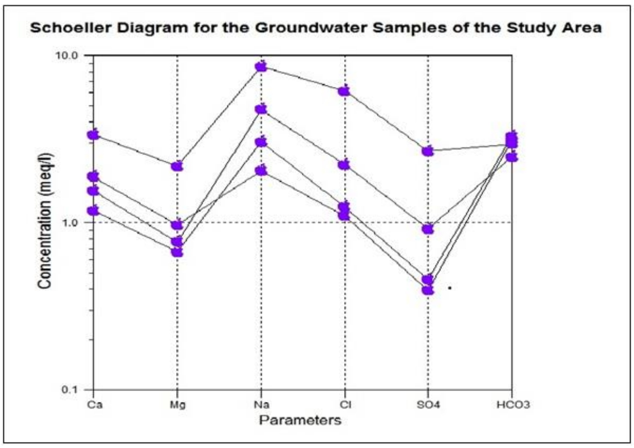

Figure 18 Schoeller diagram

4. Conclusions

The present research investigated experimentally the efficiency of the thermal insulation layer of perlite mortar to maintain the flexural performance for concrete beams reinforced by different innovative FRP bars and exposed for two hours to elevated temperatures up to 800^{o}C. The thermal progression, load-deflection curves, failure loads and failure mechanisms were presented and discussed. Based on the experimental results and observations, the following conclusions may be drawn.

- Exposing FRP RC beams to high temperatures without thermal insulation causes severe degradation in flexural strength which may lead to catastrophic failure.
- The major failure mode for the tested FRP reinforced concrete beams subjected to fire conditions without thermal insulation was controlled by FRP bar rupture.
- Thermal insulation layer of perlite mortar transformed the failure mode of the tested beams to be concrete crushing as specified by design guidelines.
- The adopted innovative thermal insulation layer of perlite mortar enhanced the ultimate load carrying capacity of RC beams reinforced by GFRP and BFRP by 202% and 180%, respectively, compared to similar uninsulated beams.
- Exceeding the critical glass transition temperature of FRP bars caused early and sudden failure of the uninsulated beams.
- The thermal insulation layer maintained the temperatures at FRP bars below the critical temperatures.

5. References

[1] Nanni A., De Luca A., Jawaheri Z. H., Reinforced concrete with FRP bars: Mechanics and Design, CRC Press, Boca Raton, FL, 2014.

[2] Urbanski M., Lapko A., Garbacz A. Investigation on concrete beams reinforced with basalt rebars as an effective alternative of conventional RC structures, Procedia Engineering 57: 1183–1191, 2013.

[3] American Concrete Institute ACI 440.1R-15, Guide for the Design and Construction of Structural Concrete Reinforced with Fiber-Reinforced Polymer (FRP) Bars, American Concrete Institute, Farmington Hills, MI 48331, 2015.

[4] Yu B., Kodur V., K., Factors governing the fire response of concrete beams reinforced with FRP rebars, Composite Structures100: 257-269, 2013.

[5] Yu, B., Kodur V., K., Fire behavior of concrete T-beams strengthened with near-surface mounted FRP reinforcement, Engineering Structures 80: 350-361, 2014.

[6] Ashrafi H., Bazli M., Najafabadi E., Oskouei A.V., The effect of mechanical and thermal properties of FRP bars on their tensile performance under elevated temperatures, Construction and Building Materials 157: 1001-1010, 2017.

[7] Hamad R.J.A., Johari M.A., Haddad R.H., Mechanical properties and bond characteristics of different fiber reinforced polymer rebars at elevated temperatures", Construction and Building Materials 142: 521-535, 2017

[8] Lu Z., Xian G., Li H., Effects of elevated temperatures on the mechanical properties of basalt fibers and BFRP plates, Construction and Building Materials 127: 1029-1036, 2015.

[9] Al-Thairy, H., Al-Hasnawi, N., H., Behavior and failure mode of GFRP bars RC beams under elevated temperature, IOP Conference Series: Materials Science and Engineering 888, 2020.

[10] Albu-Hassan N., Al-Thairy H., Experimental and numerical investigation on the behavior of hybrid concrete beams reinforced with GFRP bars after exposure to elevated temperature, Structures 28: 537-551, 2020.

[11] Dong K., Hu K., Gao W., Fire behavior of full-scale CFRP-strengthened RC beams protected with different insulation systems, Journal of Asian Architecture and Building Engineering 15(3): 581-588, 2016.

[12] Rafi M.M., Nadjai A., Ali F., Finite element modeling of carbon fiber-reinforced polymer reinforced concrete beams under elevated temperatures, ACI Structural Journal 105(6): 701-710, 2008.

[13] Salama A.E., Ghanem G.M., Abd-Elnaby S.F., El-Hefnawy A.A., Abd-Elghaffar M., Behavior of thermally protected RC beams strengthened with CFRP under dual effect of elevated temperature and loading, Housing and Building National Research Center Journal (HBRC Journal) 8(1): 26-35, 2012.

[14] Kamal O.A., Hamdy G.A., Abou-Atteya M.A., Efficiency of coating layers used for thermal protection of FRP strengthened beams," Housing and Building Research Center Journal (HBRC Journal) 10(2): 183-190, 2014.

[15] Anand N., Kiran T., Lubloy E., Mathews M.E., Kanagaraj B., Andrushia D., Flexural behavior of reinforced concrete beams with FRP bars exposed to elevated temperature, Periodica Polytechnica Civil Engineering, 2022

[16] Protchenko K., Residual fire resistance testing of basalt- and hybrid-FRP reinforced concrete beams, Materials 15: 1509, 2022.

[17] ISO 834, Fire Resistance Tests – Elements of Buildings Construction – Part I – General Requirement, International Organization for Standardization, 1999.

[18] Altunişik A.C., Akbulut Y.E., Adanur Sü., Kaya A., Günaydin M., Mostofi S., Mosallam A., Evaluating the high-temperature endurance of FRP-strengthened concrete using an innovative insulation system: Experimental investigation, Journal of Building Engineering 73(15): 106444, 2023,

[19] ES 4756-1: Cement – Part 1: composition, specifications and conformity criteria for common cements, Egyptian Organization for Standards and Quality (EOS), Cairo, Egypt, 2022.

[20] ES 1109: Aggregates for Concrete, Egyptian Organization for Standards and Quality (EOS), Cairo, Egypt, 2021.

[21] ES: 262-2: Steel for the Reinforcement of Concrete, Egyptian Organization for Standards and Quality (EOS), Cairo, Egypt, 2015.

[22] The Egyptian company for manufacturing Perlite, [Online]. Available: Expanded Perlite Construction | E.C.P. www.perlite.com.eg

[23] ASTM D7205/D7205M-06 (Reapproved 2011), Standard Test Method for Tensile Properties of Fiber Reinforced Polymer Matrix Composite Bars, Annual Book of ASTM Standards, ASTM International, West Conshohocken, PA, USA, 2011, pp. 13.

[24] ASTM E119, Standard Test Methods for Fire tests of Building Construction and Materials," ASTM International, West Conshohocken, 2015.